Supplementary Information for

Molecular Origin of the Elastic State of Aqueous Hyaluronic Acid

Giulia Giubertoni[†], Federica Burla[†], Cristina Martinez-Torres[†], Biplab Dutta[†], Galja Pletikapic[†], Eddie Pelan[‡], Yves L.A. Rezus [†], Gijsje H. Koenderink[†,] , and Huib J. Bakker[†,*]*

[†] *AMOLF, Science Park 104, 1098 XG Amsterdam, The Netherlands*

[‡]*Unilever Research and Development Vlaardingen B.V, Olivier van Noortlaan 120, Vlaardingen, 3133 AT,*

The Netherlands

Corresponding Authors:
*Gijsje H. Koenderink, and *Huib J. Bakker
G.Koenderink@amolf.nl, H.Bakker@amolf.nl

This PDF file includes:

> Data analysis methods
> Figs. S1 to S12
> Tables S1 to S2
> References for SI reference citations

Data analysis methods

Fit of the linear infrared absorption spectra at different DCl concentration. We fit the linear infrared spectra using a global fitting procedure as a function of frequency and concentration of added DCl ($[D^+_{added}]$), which is based on the minimization of the square error

$$\sum_{i,j} \left(S(\omega_j, [D^+_{added}]_i) - S^{exp}(\omega_j, [D^+_{added}]_i) \right)^2$$

(1)

where S is the fitted spectrum and S^{exp} the experimental spectrum. Assuming that the vibrational bands are Gaussian shaped, we expect that

$$\forall i, for\ \omega_{\{min\}} \leq \omega_J \leq \omega_{\{max\}}$$

$$S(\omega_j, [D^+_{added}]_i) = \sum_{k\,=\,1,2,3} c_k([D^+_{added}]_i) g_k(\omega_j) + c_{D_2O}([D^+_{added}]_i) S_{D_2O}(\omega_j)$$

(2)

where $S_{D_2O}(\omega_j)$ is the spectrum of heavy water, g_k represent the three Gaussians that describe the absorption bands of the carboxylate anion, the amide I and the carboxylic acid modes, respectively, and c_k are the Gaussians amplitudes. The heavy water spectrum is also included because we could not completely subtract the D_2O background. Examples of the fit results are shown in Fig. S3. The width and center positions of the Gaussians resulting from the fits are presented in Table S1.

Calculation of the pK$_a$ value in heavy water. We can determine the pD and the fraction of protonated/depronated carboxylic acid groups of hyaluronic acid as a function of added DCl using the acid-base equilibrium and mass balance equations:

i. $c_a = [DA] + [A^-]$
ii. $[D^+_{added}] = [DA] + [D^+]$
iii. $pK^D_{\ a} = pD^+ - \log_{10} \frac{[A^-]}{[DA]}$
iv. $pK^D_{\ w} = pD^+ + pOD^-$

(3)

The first equation represents the conservation of the analytical concentration c_a of hyaluronic acid, that at every pD has to be preserved as the sum of neutral hyaluronic acid $[DA]$ and negatively charged hyaluronic acid $[A^-]$. The second equation represents the conservation of the total concentration of D^+. The third equation is the acid-base equilibrium equation for hyaluronic acid. The fourth equation is the heavy water dissociation equilibrium, where $pK^D_{\ w}$ indicates the heavy water dissociation constant. Note that the acid dissociation constant in heavy water solutions, pK$_a{}^D$, is different from that in water solution. In order to extract the pK$_a{}^D$, we fit the fractions of $[DA]^{ext}$ and $[A^-]^{ext}$ (extracted from the global fit of the linear spectra), by using a global fitting procedure as a function of added DCl, $[D^+_{added}]$. This procedure is based on the minimization of the least-square error of the following expression:

$$\sum_i \left([DA]^{ext}([D^+_{added}]_i) - [DA]([D^+_{added}]_i, pK_a^D)\right)^2 + \sum_i \left([A^-]^{ext}([D^+_{added}]_i) - [A^-]([D^+_{added}]_i, pK_a^D)\right)^2$$

(4)

where pK_a^D is the only free parameter. $[DA], [A^-]$ are obtained by solving the system of equations in Eq.(1) with known c_a, pK_w^D as a function of $[D^+_{added}]_i$ and pK_a^D. By assuming[1] $pK_w^D = 14.95$, we obtain from the fit a value of $pK_a^D = 3.3 \pm 0.1$ that is in good agreement with the expected value from literature[2] assuming a pK$_a$ in water of 2.9 (Fig. S4).

pD to pH conversion. In case it was possible to measure the pH* of a heavy water solution, the pD was calculated with the following conversion[1]:

$$pD = pH^* + 0.44$$

(5)

The pD values can thus be converted to the pH values of a solution of water of similar acidity using[1]:

$$pH = pD * 0.929$$

(6)

In case it was not possible to measure the pH* due to the visco-elasticity of the sample, the pD was computed by solving the acid-basic equilibrium equations as a function of the known added DCl concentration, and then converted to pH by using Eq. 6. Fig.S5 demonstrates the good agreement between calculated and measured pD values.

Fit of the transient absorption spectra. The partial overlap of the –COOH diagonal peak with the cross-peak hinders a straightforward determination of the dynamics of the cross-peak. Specifically, the positive-signed *esa* band of the diagonal peak obscures the negative-signed bleach of the cross-peak. Furthermore, any heating signal originating from the interaction of the ultra-short laser pulses with the sample would either contribute or cancel out signed bands/peaks in 2D-IR spectra. Therefore, it is important to deconvolute these contributions in order to extract the dynamics emanating solely due to the cross-peaks.

The transient absorption spectrum following excitation of the ν_{COOD} vibration is obtained by averaging the signals obtained with pump frequencies between 1700 and 1760 cm^{-1} (ν_{COOD} pump-region). The transient absorption spectrum following excitation of the ν_{COOD} mode is expected to be a linear combination of four Lorentzians (two describing the cross-peaks and two describing the diagonal peaks) and a heating spectrum. However, in our case (see Fig.S8) the heating signal strongly diminishes the amplitude of the *esa* band. As a consequence, our fitting routine is not able to disentangle the contribution of the positive-signed *esa* of the cross-peak. We thus use three Lorentzians, and we describe the transient absorption spectrum:

$$\forall i, for\ \omega_{min}^{probe} \le \omega_j^{probe} \le \omega_{max}^{probe}$$

$$S(\nu_j^{probe}, t_i) = \sum_{k=1}^{3} c_k(t_i) l_k(\omega_j^{probe}) + c_h(t_i) h(\omega_j^{probe})$$

(7)

3

The heating spectrum is taken directly from the transient absorption spectrum at 50 ps, when the vibrational dynamics is over (Fig. S8). We obtain a width for this Lorentzian of 39 ±5 cm^{-1} and a central frequency of 1639 cm^{-1}. The width and center position of the cross-peak and the width of the bleach of the diagonal peak are constrained in a global fit to the transient absorption spectra at all delays following excitation of the ν_{COOD} mode. The global fitting procedure is performed as a function of probe frequency and delay time and it is based on the minimization of the least-square error using the following expression

$$\sum_{ij} \left(S\left(\omega_j^{probe}, t_i \right) - S^{exp}\left(\omega_j^{probe}, t_i \right) \right)^2$$

(8)

where S^{exp} represents the measured transient absorption spectrum. The resulting central frequencies and widths of the Lorentzians are presented in Table S2.

The same global fitting routine is applied to determine the amplitudes of the Lorentzian in experiments where we recorded the transient absorption spectra separately with the polarization of the probe pulses parallel and perpendicular with respect to the pump pulse. By using the Lorentzian amplitudes extracted at every time t_i for parallel - $c^{par}(t_i)$ - and perpendicular - $c^{per}(t_i)$ - polarizations, we can then calculate the anisotropy $R(t_i)$, which is defined as[4]:

$$R(t_i) = \frac{c^{par}(t_i) - c^{per}(t_i)}{c^{par}(t_i) + 2c^{per}(t_i)}$$

(9)

Fig.S10 reports the obtained anisotropies. We can extract the angle between the direction of the transition dipole moments at time 0 and time t_i by exploiting the following relation between anisotropy and the angle [5]:

$$R(t_i) = \frac{3\cos^2 \theta(t_i) - 1}{5}$$

(10)

In case of the cross-peak, the extracted angles reflect the relative orientation between the carboxylic acid and amide dipole moments (inset Fig. S10).

Relaxation model. We model the delay-time dependence of the cross-peak of the ν_{COOD} mode and the $\nu_{Am,I}$ mode (amide I mode) as the result of the relaxation of two carboxylic acid species. One species, with population $N_{th}(t)$, relaxes by energy transfer to lower-frequency modes. These lower-frequency modes are anharmonically coupled to the amide modes. The other carboxylic acid species, with population $N_{ent}(t)$, relaxes via energy transfer to a nearby amide I vibration (*ent*). We thus write the cross-peak transient signal as:

$$\Delta\alpha_{cp}(\omega^{probe}, t) = -2\sigma_{AM.I}\left(\omega^{probe} \right)\left(w\left(\beta_{AM.I,LFM} \right) * N_{th}(t) + N_{ent.}(t) \right)$$

(11)

4

where $\sigma_{AM.I}$ is the amide I cross-section and $w(\beta_{AM.I,LFM})$, a coupling-dependent weighing factor, is introduced to take care of the coupling-dependent energy transfer pathway. Note that $\beta_{AM.I,LFM}$ denotes the vibrational coupling between the amide I and low frequency modes. $N_{th}(t)$ and $N_{ent.}(t)$ can be described as follows:

$$N_{th}(t) = N_{th}(t=0)\left(\frac{T_{1LFM}}{T_{1COOD} - T_{1LFM}}\right)\left(e^{-t/T_{1COOD}} - e^{-t/T_{1LFM}}\right)$$

(12)

and

$$N_{ent}(t) = N_{ent}(t=0)\left(\frac{T_{1AM.I}}{T_{ent} - T_{1AM.I}}\right)\left(e^{-t/T_{ent}} - e^{-t/T_{1AM.I}}\right)$$

(13)

where T_{1COOD} is the lifetime of the carboxylic acid mode (0.65 ± 0.1 ps), $T_{1AM.I}$ is the lifetime of the amide I mode (0.65 ± 0.1 ps) and T_{1LFM} is the lifetime of the low frequency modes extracted from a fit to the cross-peak signal of the ν_{COOD} mode and the $\nu_{Am,II}$ mode (amide II mode). By normalizing the $\Delta\alpha_{cp}(\omega^{probe},t)$ to $\Delta\alpha_{COOD}(\omega^{probe},\bar{t}=200\,fs)$ we obtain from Eq.11 that

$$\frac{\Delta\alpha_{cp}(\omega^{probe},t)}{\Delta\alpha_{COOD}(\omega^{probe},\bar{t})} = \frac{-2\sigma_{AM.I}(\omega^{probe})(w(\beta_{AM.I,LFM}),N_{th}(t)+N_{ent}(t))}{-2\sigma_{COOD,bl}(\omega^{probe})N_{COOD}(\bar{t})} =$$

$$= \frac{\sigma_{AM.I}(\omega^{probe})}{\sigma_{COOD}(\omega^{probe})}\frac{(w(\beta_{AM.I,LFM}),N_{th}(t)+N_{ent.}(t))}{N_{COOD}(\bar{t})} =$$

(14)

and by using Eq.12 and Eq.13

$$= c_{th.}\cdot\left(\frac{T_{1LFM}}{T_{1COOD} - T_{1LFM}}\right)\left(e^{-t/T_{1COOD}} - e^{-t/T_{1LFM}}\right) + c_{ent.}\left(\frac{T_{1AM.I}}{T_{ent} - T_{1AM.I}}\right)\left(e^{-t/T_{ent}} - e^{-t/T_{1AM.I}}\right),$$

(15)

where $c_{th.} \equiv \dfrac{\sigma_{AM.I}(\omega^{probe})\,w(\beta_{AM.I,LFM}),}{\sigma_{COOD}(\omega^{probe})}\dfrac{N_{th}(\bar{t})}{N_{COOD}(\bar{t})}$ and $c_{ent.} \equiv \dfrac{\sigma_{AM.I}(\omega^{probe})}{\sigma_{COOD}(\omega^{probe})}\dfrac{N_{ent.}(\bar{t})}{N_{COOD}(\bar{t})}$

T_{ent}, $c_{th.}$ and $c_{ent.}$ are the only free parameters of the fit to the experimental cross-peak signals of the ν_{COOD} mode and the $\nu_{Am,I}$ mode (amide I mode). In Figure S8 we show the dynamics of the diagonal COOD peak both for the putty state (pH=2.5) and the solution state at pH=2.9. The dynamics are very similar showing a T_{1COOD} of 0.65±0.1 ps.

2DIR study of the amide-COO⁻ interaction. We studied the interaction between the amide and carboxylate anion groups with 2DIR spectroscopy. The most intense modes of these two groups, the amide I ($\nu_{AM,I}$) and the anti-symmetric stretching vibrations ($\nu_{ant,COO}$⁻), absorb at ~1640 and ~1608 cm⁻¹, respectively, and overlap in both linear and 2DIR spectra. We studied the $\nu_{AM,I}$ - $\nu_{ant,COO}$⁻ cross-peak signal and its pH dependence with two different methods.

In the first method, we measure 2D-IR spectra with parallel and perpendicular polarization of the excitation and detection pulses at pH=1.9 (with a concentration of COO⁻ <5%), pH=2.5 (with a concentration of COO⁻ of ~20%), and pH=2.9 (with a concentration of COO⁻ of ~50%). We construct the isotropic 2DIR spectra at pH=1.9, pH=2.5, and pH=2.9, at a time delay of 0.3 ps (Fig.S11a-b-c). We then normalize all the 2DIR spectra to the maximum intensity observed for a pump frequency of 1645 cm⁻¹ (at this frequency the 2D-IR signal is completely dominated by the amide I vibration). We then subtract the 2DIR spectrum at pH=1.9 from the 2DIR spectra at pH=2.5 and pH=2.9. This allows us to compare the diagonal and cross-peak signals involving the $\nu_{ant,COO}$⁻ mode at pH=2.5 and pH=2.9, as the amide I signal can be assumed to be pH independent. The resulting difference spectra are denoted as $sub_{pH=2.5}$ (Figure S11d) and $sub_{pH=2.9}$ (Figure S9e). The difference 2DIR spectra show a strong diagonal signal of the $\nu_{ant,COO}$⁻ mode, and a weaker off-diagonal signal at a pump frequency of ~1640 cm⁻¹ and a probe frequency of ~1610 cm⁻¹. The diagonal signal is stronger for the $sub_{pH=2.9}$ than for the $sub_{pH=2.5}$ 2DIR spectrum, because of the higher concentration of COO⁻ at pH=2.9. The off-diagonal signal represents the $\nu_{AM,I}$ - $\nu_{ant,COO}$⁻ cross-peak signal. We integrate this off-diagonal signal over a range of pump frequencies between 1637 cm⁻¹ and 1650 cm⁻¹ to eliminate possible effects of spectral diffusion. The resulting signal is shown as a function of the detection frequency in Figure S11f. The signals are normalized to the diagonal signal of the $\nu_{ant,COO}$⁻ mode at 1610 cm⁻¹. We observe that the cross-peak signal (pumping $\nu_{AM,I}$ at ~1640 cm⁻¹ and probing $\nu_{ant,COO}$⁻ at ~1610 cm⁻¹) is stronger at pH=2.5 than at pH=2.9. This difference shows that the interaction between the amide and carboxylate anion groups is enhanced at pH=2.5 in comparison to pH=2.9.

In a second method we determined the strength of the cross-peak signal at different pH values by subtracting the parallel 2D-IR spectrum from three times the perpendicular 2D-IR spectrum, both at pH=2.5 (Figure 5a of the manuscript) and at pH=2.9 (Figure S12). This procedure reveals the cross-peak signals of the $\nu_{AM,I}$ and $\nu_{ant,COO}$⁻ vibrations, as all diagonal signals of $\nu_{AM,I}$ and $\nu_{ant,COO}$⁻ will be strongly suppressed. From the resulting difference 2D-IR spectra we subsequently construct transient absorption spectra, in which we average over the excitation frequency interval between 1600 and 1620 cm⁻¹ (excitation of $\nu_{ant,COO}$⁻). These spectra (shown in Figure 5b of the manuscript) contain a clear $\nu_{AM,I}$ - $\nu_{ant,COO}$⁻ cross-peak signal near 1635 cm⁻¹ (detection of $\nu_{AM,I}$). To compare the fraction of COO⁻ groups that interacts with an amide group at pH=2.5 with that at pH=2.9, we normalize the transient absorption signals at pH=2.5 and 2.9 of Fig. 5b of the manuscript to the diagonal signals of the $\nu_{ant,COO}$⁻ mode at 1610 cm⁻¹ at these pH values (Figs. S11d and S11e). The cross-peak signal near 1635 cm⁻¹ is stronger at pH=2.5 than at pH=2.9, showing the enhanced interaction between the COO⁻ and amide groups at pH=2.5 (putty state).

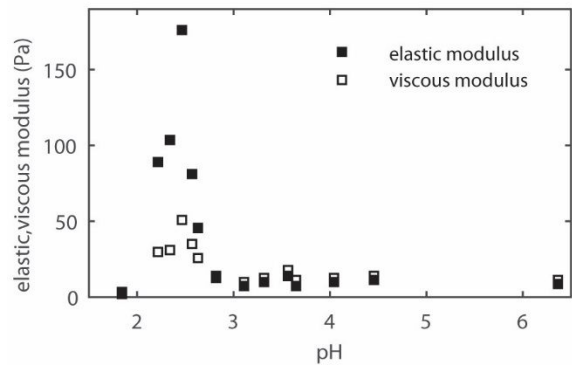Fig.S1: Picture of the solution and putty states at a hyaluronic acid concentration of 10 mg/ml.

Fig.S2 : pH-dependence of the viscous and elastic modulus of hyaluronic acid solutions at 10 mg/ml in H_2O.
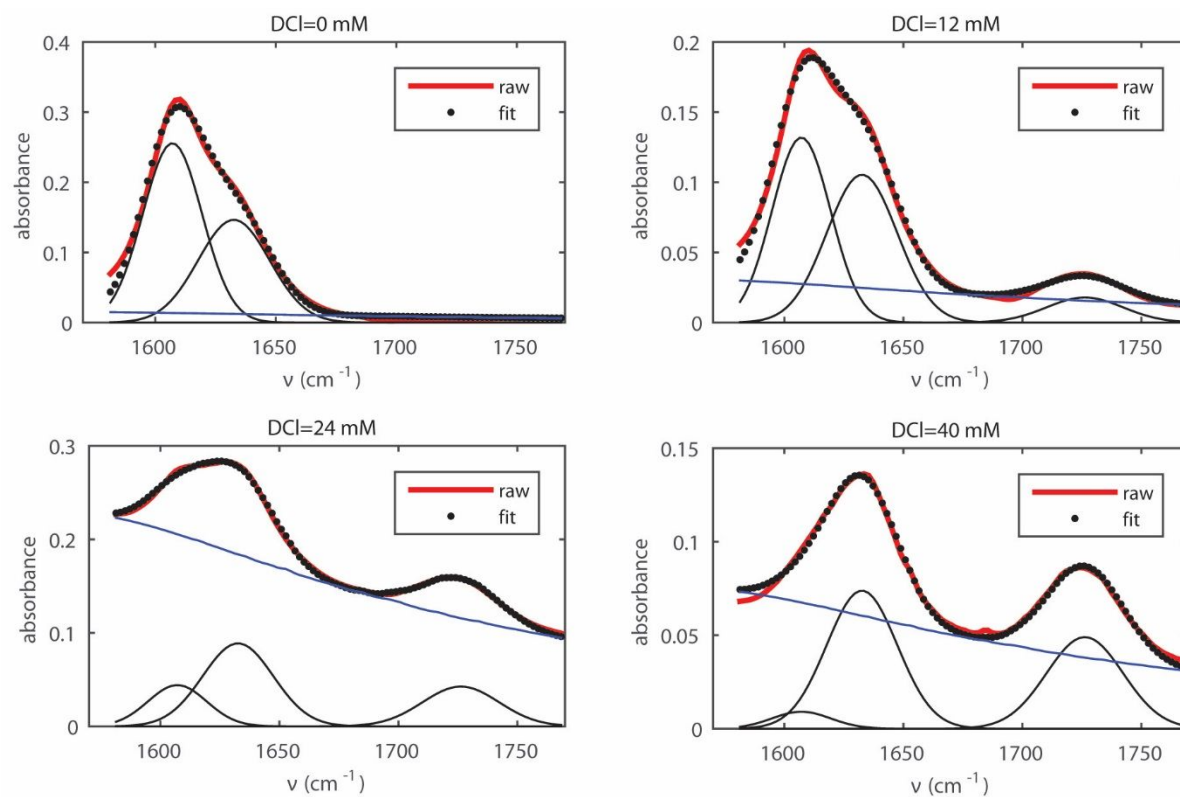
Fig.S3: Measured and fitted linear absorption spectra of a solution of hyaluronic acid of 10 mg/ml in heavy water for different DCl concentrations. Blue lines represent the heavy water background spectrum, whilst the black lines show the Gaussian-shaped vibrational bands.
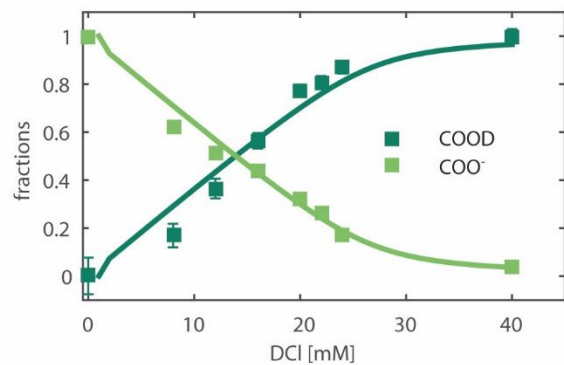
Fig.S4: Normalized fractions of COOD and COO⁻ obtained from fitting the IR-spectra as a function of added DCl. The thick lines are fits to the basic-acid equilibrium model (Eq. 1) assuming a $\mathbf{pK_a^D} = 3.3$.
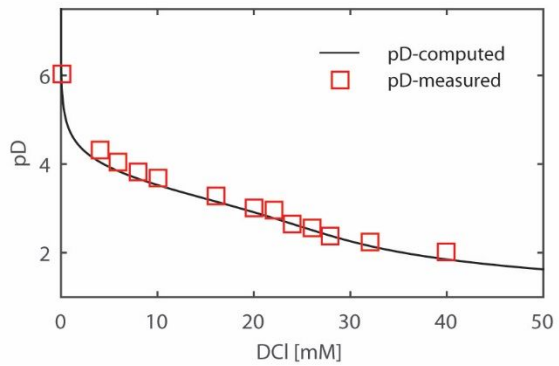
Fig.S5: Comparison between expected pD values obtained by solving the acid-basic equilibrium with $pK^D_a = 3.3$ and the measured pD values as a function of added DCl concentration.
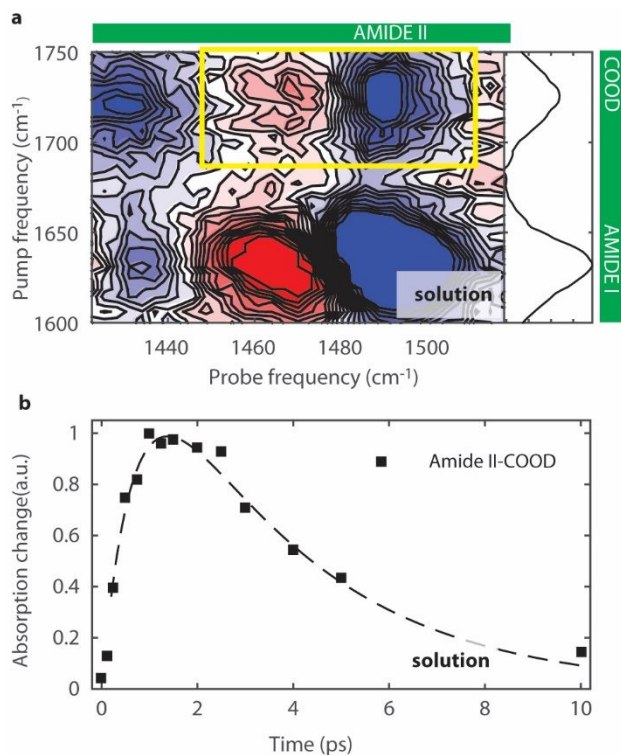
Fig.S6: a) Isotropic 2D-IR spectrum for hyaluronic acid in D_2O solutions at a concentration of 15 mg/ml in the solution state. Spectrum was collected at a delay time of 1.5 ps. The pump and probe spectra are centered at 1680 cm^{-1} (AMIDE I region) and 1450 cm^{-1} (AMIDE II region) respectively. The cross-peak, which appears in the region indicated by the yellow rectangle, reveals a vibrational interaction between $\nu_{AM.II}$ and ν_{COOD}. The additional cross-peaks observed at a probe frequency around 1440 cm^{-1} are due to vibrational coupling with the bending modes of the –COH and –CCH groups of the N-acetyl-galactosamine and glucurononic acid moieties. Due to the low signal-to-noise at pH 2.5, it was not possible to perform the same experiment in the putty state. b) Decay trace for the cross-peak in the $\nu_{AM.II}$ vibrational region normalized to the minimum intensity. The decay is fit to a two-step consecutive reaction model, shown by the dashed line. The time constants are 0.7 ps for the initial signal growth and 3.3 ps for the decay. The build-up time constant is comparable to the vibrational relaxation time $T_{1.COOD}$ of the COOD parent-mode of 0.65±0.1 ps. The decay time τ_2 is much longer than the vibrational lifetimes of the COOD, amide I, and amide II vibrations. This result indicates that the ν_{COOD} - $\nu_{AM.II}$ cross-peak results from the transient excitation of low-frequency modes within the hyaluronic acid chain that affect the absorption spectrum of the amide II vibration. The low-frequency modes become excited as a result of the vibrational relaxation of ν_{COOD}, thus explaining the build-up of the cross-peak signal with τ_1 of ~0.7 ps. The cross-peak signal decays when the low-frequency modes transfer their energy to other modes, for instance to the modes of water. The time constant τ_2 thus represents the time constant $T_{1.LFM}$ of the relaxation of the low-frequency modes.
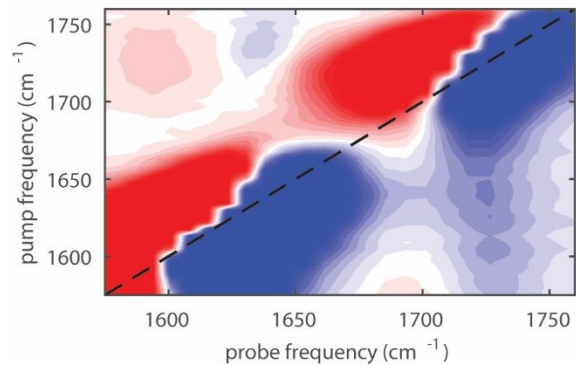
Fig.S7: Parallel 2DIR spectrum at 0.3 ps for a solution of hyaluronic acid at the putty state (pH=2.5) at 20 mg/ml. Colour scale represents 2D-IR signal normalized to the cross-peak intensity. It is also possible to observe the elongated spectral shape of the carbonyl , which affects the upward cross-peak signal.
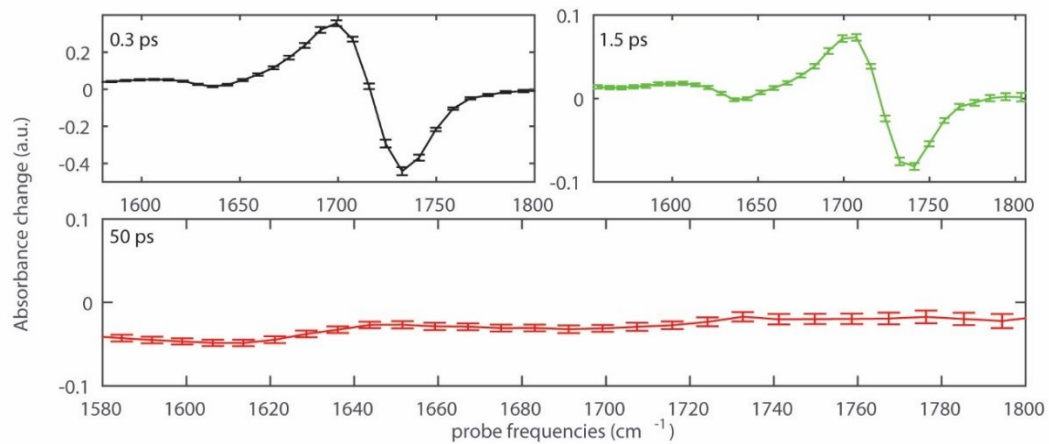
Fig.S8: Transient absorption spectra obtained by averaging over the 2DIR signals obtained with pump frequencies between 1700 cm^{-1} and 1760 cm^{-1} at three different delay times (see legends).
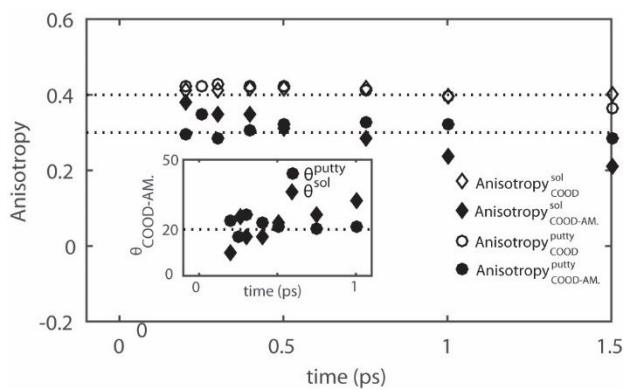
Fig.S9: Anisotropy of the bleach of the cross-peak and of the diagonal peak of the carbonyl vibration of the –COOD group extracted by fitting parallel and perpendicular signal to the pump-slices. In the inset, the extracted angle from the cross-peak anisotropy. By averaging over 6 different measurements, we obtain an angle of 20° ± 5°.
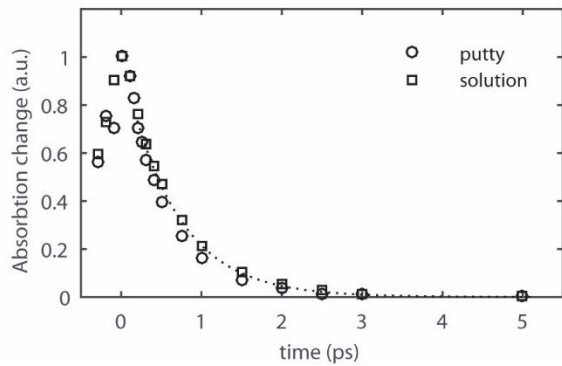
15

Fig.S10: Normalized decay traces of the bleach of the COOD vibration for the putty and solution state (see legend), extracted at a pump frequency of 1721 cm^{-1} and probe frequency of 1730 cm^{-1}.
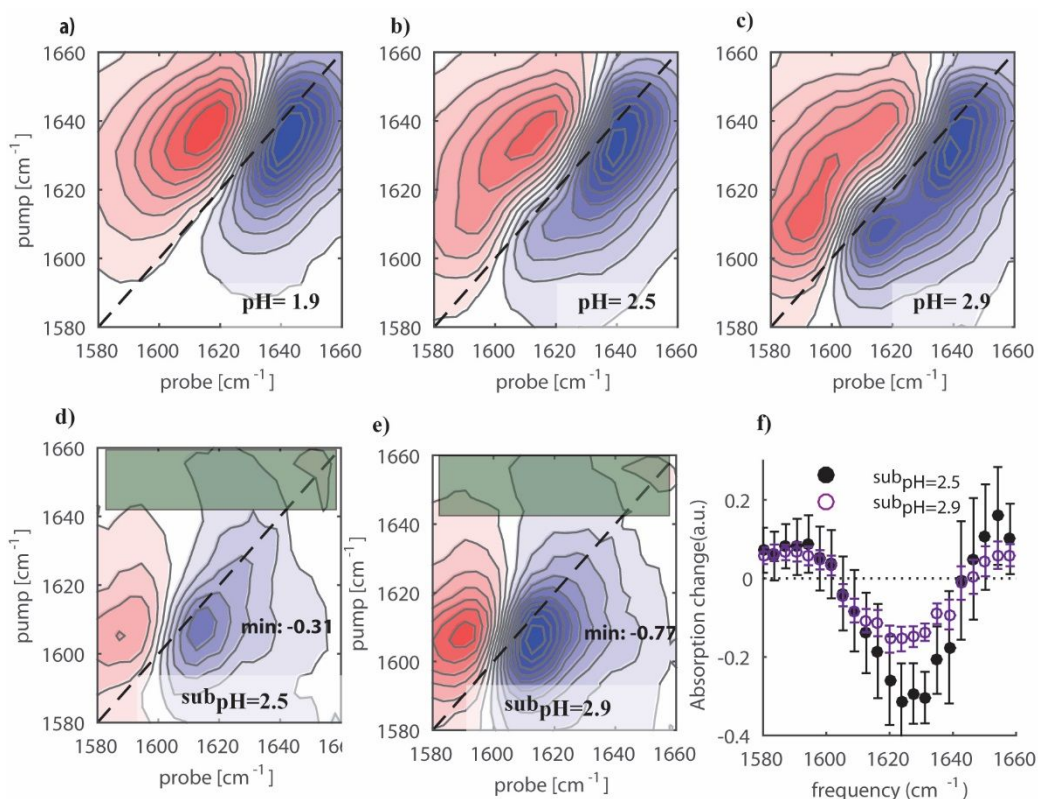
Fig.S11: 2DIR spectra of hyaluronic acid at a concentration of 20 mg/ml at pH=1.9, pH=2.5 and pH=2.9 in figure **a)**, **b)** and **c)**. **d)** and **e)** are obtained by subtracting **a)** from **b)** and **a)** from **c),** respectively, after normalizing the 2DIR spectra to the minimum intensity along the pump frequency around 1645 cm^{-1}. We will refer to the subtracted 2DIR spectra in **d)** and **f)** as $sub_{pH=2.5}$ and $sub_{pH=2.9}$, respectively. By doing such normalization and subtraction, it is possible to cancel the presence of the intense amide I vibration, and thus to observe eventual off-diagonal features. In figure **f)** we report the pump-slices obtained by averaging over the pump frequencies between 1637 cm^{-1} and 1650 cm^{-1} (which is the region highlighted by a dark green rectangle) in the 2DIR spectra shown in figures **d)** and **e))**. The slices are normalized to the respective bleaches of the COO^- vibration at 1610 cm^{-1} of Figures d) and e). At pH=2.5 we observe a larger negative absorption change around 1620 cm^{-1} in comparison to pH=2.9. This larger negative absorption change indicates that more amide and carboxylate anion groups are interacting with each other at pH=2.5 than at pH=2.9.
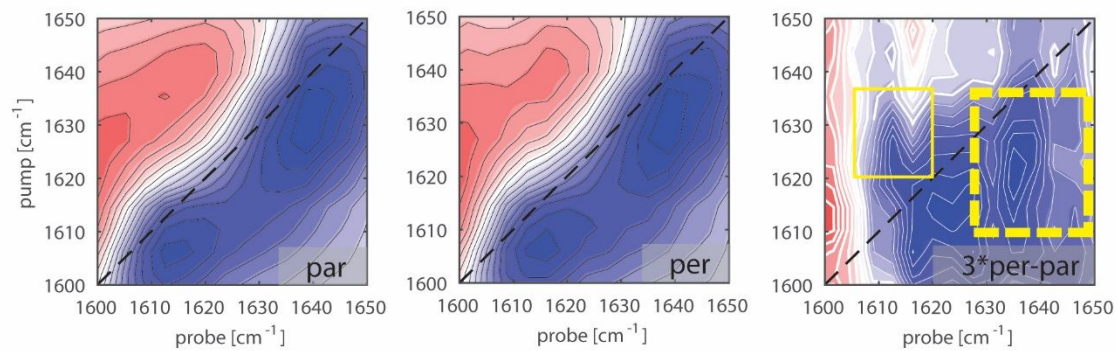
17

Fig.S12: 2DIR spectra of a solution of hyaluronic acid at pH=2.9 at a concentration of 20 mg/m at a waiting time of 0.3 ps.
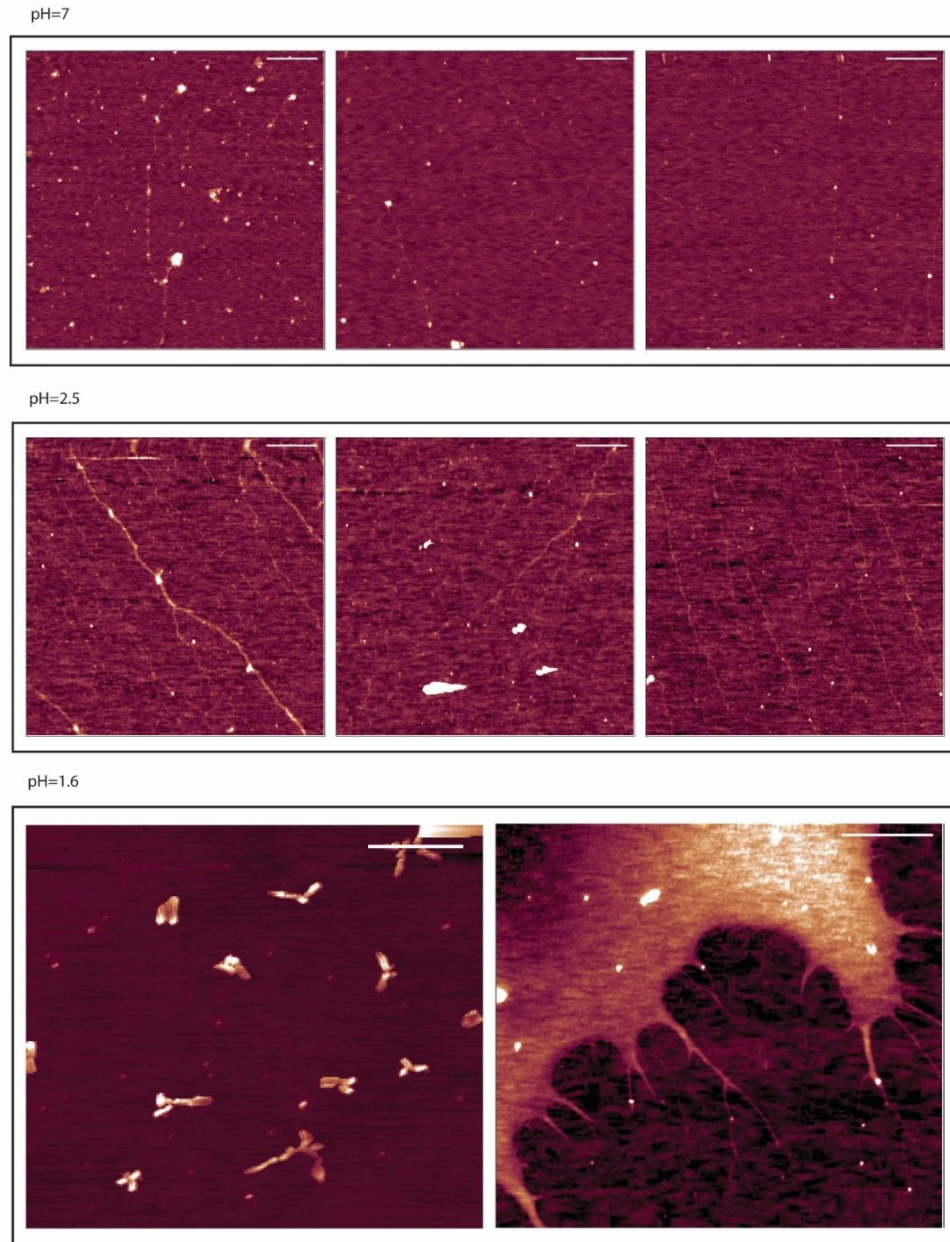
pH=7

pH=2.5

pH=1.6

Fig.S13: AFM height images of hyaluronic acid filaments at pH 7, pH 2.5 and pH 1.6. The images are colour coded from 0 nm (dark red) to 1.2 nm (white) for AFM height images at pH 7 and pH 2.5. Scale bar: 500 nm. Colour coded from 0 (dark red) to 45 nm (white) for the left image at pH=1.6AFM height image.

Table S1: Central frequencies and widths of the Gaussians of the fitted linear absorption spectra.

	$\nu(cm^{-1})$	FWHM (cm^{-1})
ν_{ant,COO^-}	1607	29
ν_{AMI}	1633	35
ν_{COOD}	1726	38

Table S2: Parameters of the three Lorentzians representing the bleaching of the ν_{COOD} mode, the excited-state absorption of the ν_{COOD} mode, and the bleaching of the cross peak signal between the ν_{COOD} mode and the $\nu_{Am,I}$ mode in the transient absorption spectrum following excitation of the ν_{COOD} mode. The errors are the standard deviations computed by averaging over at least three different independent measurements.

$\nu_{COOD, ESA}$		$\nu_{COOD,BLEACH}$*	$\nu_{AMIDE\ I,ESA}$		$\nu_{AMIDE\ I,BLEACH}$*	$\nu_{COOD-AMIDE\ I, BLEACH}^{+}$
ν_0 (cm^{-1})	FWHM (cm^{-1})	ν_0 (cm^{-1})	FWHM (cm^{-1})	ν_0(cm^{-1})	ν_0(cm^{-1})	FWHM (cm^{-1})
1703±1	47±2	1731±1	48±2	1619±1	1639±1	39±4

*FWHM is constrained by using the value extracted by the fit of linear spectra
$^{+}\nu_0$ is constrained at 1639 cm^{-1}

References:

1.   Kręžel, A. & Bal, W. A formula for correlating pKa values determined in D2O and H2O. *J. Inorg. Biochem.* **98,** 161–166 (2004).
2.   Mora-Diez, N., Egorova, Y., Plommer, H. & Tremaine, P. R. Theoretical study of deuterium isotope effects on acid–base equilibria under ambient and hydrothermal conditions. *RSC Adv.* **5,** 9097–9109 (2015).
3.   Selig, O., Siffels, R. & Rezus, Y. L. A. Ultrasensitive Ultrafast Vibrational Spectroscopy Employing the Near Field of Gold Nanoantennas. *Phys. Rev. Lett.* **114,** 233004 (2015).
4.   Duxbury, G. *Concepts and Methods of 2D Infrared Spectroscopy, by Peter Hamm and Martin Zanni. Cambridge University Press* **52,** (Cambridge University Press, 2011).
5.   Bodis, P. *et al.* Two-dimensional vibrational spectroscopy of rotaxane-based molecular machines. *Acc. Chem. Res.* **42,** 1462–1469 (2009).